8-2010

Optimizing performance of plasmonic devices for photonic circuits

Tiberiu Rosenzveig
University of Iceland

Petur Gordon Hermannsson
University of Iceland

Alexandra Boltasseva
Birck Nanotechnology Center, Purdue University, aeb@purdue.edu

Kristjan Leosson
University of Iceland

Appl Phys A (2010) 100: 341–346
DOI 10.1007/s00339-010-5862-2

Applied Physics A
Materials Science & Processing

Optimizing performance of plasmonic devices for photonic circuits

Tiberiu Rosenzveig · Petur Gordon Hermannsson · Alexandra Boltasseva · Kristjan Leosson

Received: 13 August 2009 / Accepted: 1 June 2010 / Published online: 22 June 2010

Abstract We demonstrate the feasibility of fabricating thermo-optic plasmonic devices for variable optical attenuation and/or low-frequency (kHz) signal modulation. Results of finite-element simulations and experimental characterization of prototype devices indicate that a plasmonic device can reach specifications similar to or better than commercially available thermo-optic integrated optical components. Specifically, we have considered the insertion loss, power consumption, footprint, polarization-dependent loss, extinction ratio, and frequency response of the plasmonic devices, in addition to fabrication and material-related issues. The most serious fabrication challenge is to realize metallic nanowire waveguides with a sufficiently accurate cross-section to ensure low polarization-dependent loss at high extinction ratios.

1 Introduction

Surface plasmon polaritons (SPPs) are often associated with sub-wavelength confinement of light and a number of passive and active devices based on guiding of highly confined SPPs have been proposed [1]. It is, however, also possible to use so-called long-range surface plasmon polariton (LRSPP) waveguides [2–4] with weaker confinement to realize individual optical components that maintain compatibility with current mode-size standards but can, in some cases, have a significantly smaller footprint than their dielectric counterparts [5, 6]. Nevertheless, several challenges have to be overcome in order to compete with glass or polymer-based integrated optics, mainly those of insertion loss and polarization dependence. Other factors such as response time, power consumption, dynamic range, scalability and fabrication tolerances also have to be critically assessed.

In the present paper, we address these issues for plasmonic waveguide devices designed for variable optical attenuation and/or low-frequency modulation at telecom wavelengths, using finite-element simulations and experimental characterization.

2 Target specifications

A variable optical attenuator (VOA) attenuates the intensity of an optical input in a controlled manner. VOAs are important components of modern optical networks where they are used for regulating power levels to protect receivers and prevent saturation, gain flattening in wavelength division multiplexed networks, dynamic channel equalization in cross-connected nodes, channel blanking and channel labeling for network monitoring, etc.

As a reference component, we consider a commercially available thermo-optic polymer-based integrated variable optical attenuator supplied by Enablence Technologies Inc. (previously DuPont Photonics).[1] According to the manufac-

T. Rosenzveig · P.G. Hermannsson · K. Leosson (✉)
Science Institute, University of Iceland, Dunhagi 3, 107 Reykjavik, Iceland
e-mail: kleos@hi.is
Fax: +354-552-8911

A. Boltasseva
School of Electrical and Computer Engineering, Birck Nanotechnology Center, Purdue University, West Lafayette, IN 47907, USA

A. Boltasseva
DTU Fotonik, Department of Photonics Engineering, Nano·DTU, Technical University of Denmark, DTU Building 343, 2800 Kongens Lyngby, Denmark

[1] http://www.enablence.com/media/pdf/enablence_ivoa_datasheet.pdf.

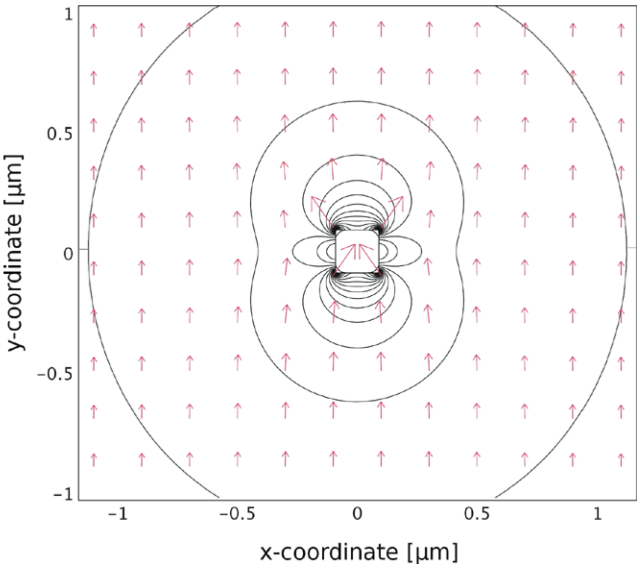

Fig. 1 The calculated magnitude and direction of the electric field of the predominantly y-polarized $E^{(0,1)}$ mode propagating along a 180 nm × 180 nm gold wire embedded in a dielectric cladding. The x-polarized $E^{(1,0)}$ mode is obtained by 90° rotation

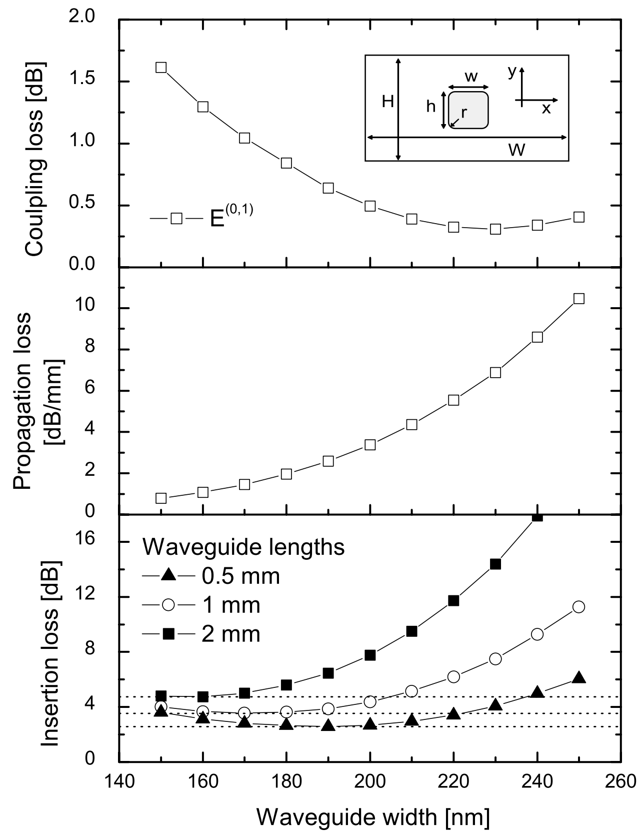

Fig. 2 Calculated coupling loss, propagation loss and fiber-to-fiber insertion loss for 0.5-, 1- and 2-mm long gold nanowire waveguides in a 20 μm thick cladding layer at $\lambda = 1550$ nm. Similar values are obtained for both polarizations, so only the $E^{(0,1)}$ results are shown. The *inset* in the top panel schematically shows the simulated device geometry

turers datasheet, the packaged device has an off-state insertion loss of 1.3 dB, extinction ratio of 20 dB, response time of 3 ms, power consumption of 40 mW/channel and PDL ≤ 0.7 dB over the attenuation range. Although not stated in the datasheet, it can be assumed that the devices operate on an interferometric principle, with the actual device length being around 10 mm [7].

3 Waveguide structure

Polarization-dependent loss (PDL) is one of the key features of devices in the optical network where polarization generally changes randomly with time. Components based on conventional LRSPP waveguides consisting of thin metal stripes embedded in a homogeneous dielectric environment only support guiding of light polarized perpendicular to the stripe surface. Square cross-section nanowire waveguides, however, were proposed [8] and experimentally verified [9] to serve as polarization-independent plasmonic waveguides. A metallic wire with a square cross-section in an uniform dielectric environment supports long-range supermodes (combinations of four corner modes) with the electric field oriented predominantly along the x or y directions, as shown in Fig. 1. Following Jung et al. [10], we label these modes $E^{(1,0)}$ and $E^{(0,1)}$, respectively. In practical situations, the dielectric cladding will have a finite thickness, which may influence the plasmonic modes as discussed in Sec. 4.

4 Insertion loss

Effective mode indices and field distributions were determined by finite-element analysis[2] of plasmonic waveguides consisting of square-symmetric gold nanowires embedded in a polymer cladding, similar to experimentally fabricated devices [6]. Modeling was performed using a free-space wavelength of 1550 nm. The gold nanowire ($\tilde{n} = 0.52 + 10.7i$ [11]) was surrounded by a dielectric cladding ($n = 1.535$), bounded by air on all sides as shown in the inset of Fig. 2. For each nanowire side length, the resulting mode profile was used to determine the minimum end-fire coupling loss by calculating the overlap with the Gaussian fiber mode of a single-mode fiber (SMF28) having a mode-field diameter of 10.5 μm.

Propagation loss due to absorption in the metal (neglecting scattering, absorption in the polymer and radiation leakage) was derived from the calculated effective mode indices. The results are shown in Fig. 2 along with the insertion

[2] Comsol Multiphysics (RF module), http://www.comsol.com.

loss (2 × CL + PL × length) of 0.5-, 1- and 2-mm long straight waveguide components with 20 µm cladding thickness. A minimum coupling loss of 0.31 dB (corresponding to a mode overlap of 93%) was obtained for a waveguide having 230-nm side length. However, for this side length, the propagation loss has an unacceptably large value of 6 dB/mm. For short waveguide sections (0.5–1 mm), the optimum wire side length is in the range 170–190 nm. Nevertheless, the lowest theoretical insertion loss for a 0.5-mm device (around 3 dB), still exceeds our target specifications.

In order to further tailor the mode size of the plasmonic nanowire modes, additional confinement can be provided by modifying the cladding geometry, as described in detail in Ref. [12]. For narrow wires in particular, the increased confinement from a thinner cladding substantially decreases the coupling loss while causing only a modest increase in propagation loss. Furthermore, performance can be optimized using a hybrid dielectric-plasmonic waveguide geometry with the nanowire embedded in a square dielectric core with a side length of about 16 µm (in air). This results in a minimum insertion loss close to 1.4 dB for a 0.5-mm device length. More realistically, the hybrid plasmonic-dielectric waveguide should be embedded in a low-index polymer (e.g. Cytop or Teflon AF) which will give a slightly different optimum dielectric core size.

Previously, short (1–2 mm) VOA devices with high extinction ratios have been realized [6] and we propose that such devices can be made even shorter in order to bring insertion losses down to 1–2 dB. It remains to be seen, however, how the added confinement and reduced length affect the power consumption and achievable extinction ratio of the VOA device.

5 Extinction mechanism

The operation of the currently investigated plasmonic VOA makes use of the negative thermo-optic coefficient of polymers [13]. By passing electrical current through the waveguide core, the effective refractive index of the guided mode is changed due to the temperature-dependent refractive index of the cladding material. The exact extinction mechanism, however, has not previously been determined. By simulating the heat flow in our nanowire devices (see inset of Fig. 3) and determining the resulting temperature and refractive index profiles, we followed the change in the eigenmodes of the structure as heating power was increased. The temperature dependence of the dielectric function of gold [14] was also included in the model. As expected, the long-range modes expand upon heating and become slightly asymmetric due to the asymmetric cooling conditions above and below the cladding (here, the presence of a substrate acting as an effective heat sink was taken into account, while

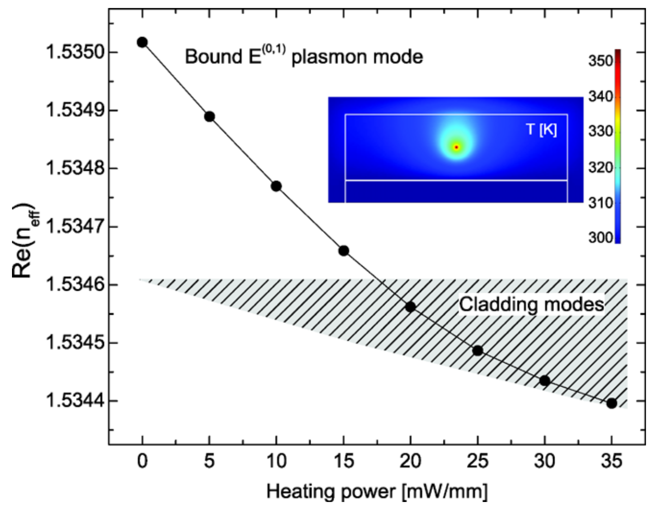

Fig. 3 The real part of the effective index for the $E^{(0,1)}$ mode versus electrical heating power for a gold nanowire. The grey area corresponds to the refractive index of the cladding layer which has a temperature-induced index gradient. The calculated temperature profile (color) is shown in the *inset*, corresponding to a heating power of 20 mW/mm

cooling at the top surface was treated as simple heat conduction to still air). The effective refractive index of the guided mode drops and eventually crosses into the regime corresponding to freely propagating modes in the cladding which develops a significant index gradient due to the temperature profile.

By calculating propagation and coupling losses for an electrically heated 180 nm × 180 nm wire, we can determine whether changes in these parameters fully account for the extinction ratio observed in our VOA devices. The calculation assumes an abrupt (non-adiabatic) coupling to the heated section which is reasonable since the temperature gradient along the propagation direction from heated to unheated sections of the waveguide only extends over a few wavelengths. In general, the coupling loss increases with heating power while propagation loss decreases, as shown in Fig. 4. The combined effect, however, only amounts to a 4–6 dB extinction at 30 mW/mm heating power for 1-mm long devices, whereas 10–15 dB are observed experimentally in wires with similar dimensions [6] at the corresponding power levels. We therefore conclude that scattering of plasmons to radiative cladding modes contributes substantially to the extinction. We have shown experimentally that extinction ratios significantly higher than our target specification can be realized, even in devices as short as 1 mm [6].

6 Fabrication issues; symmetry, adhesion layers, hysteresis

Geometric tolerances for realizing polarization-independent waveguides were considered in Ref. [12], where it was

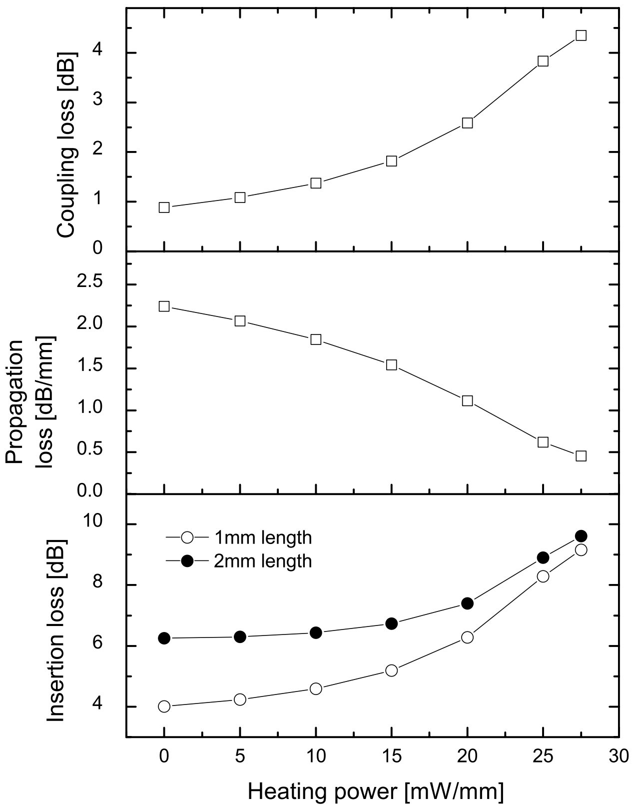

Fig. 4 Effect of heating on coupling loss and propagation loss in nanowire waveguides. The total insertion loss increases with heating, but the change is considerably smaller than observed in experiment

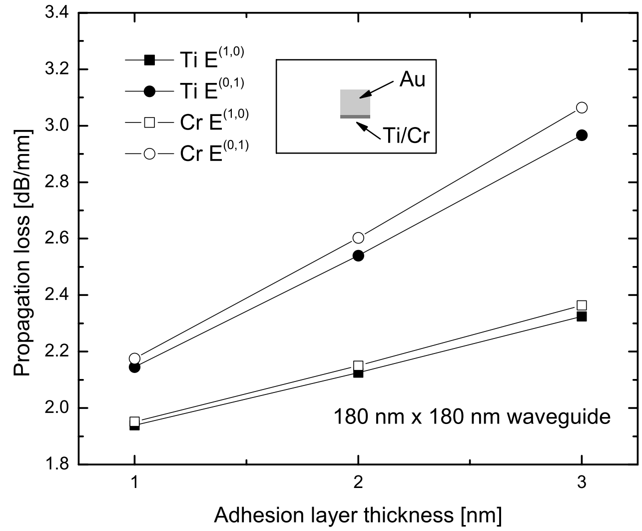

Fig. 5 Calculated effect of adhesion layers on propagation loss and polarization dependence in a 1-mm long symmetric nanowire waveguide

found that a small deviation from square symmetry will result in significantly polarization-dependent propagation and coupling loss, although the two contributions partially cancel out. Simulation results indicate that for 1-mm long devices, the total PDL is < 0.6 dB, for up to $\pm 10\%$ asymmetry, which is within acceptable limits from the fabrication point of view. Experiments show, however, that the PDL at high extinction ratios depends much more critically on wire dimensions [6]. In order to meet target specifications for PDL over the whole attenuation range, therefore, asymmetry of the wires presumably has to be kept below 2%.

Another potential source of polarization dependence is the presence of a thin adhesion layer, required to avoid delamination of the waveguides from the polymer substrate during the lift-off process. Adhesion layers were found to have a substantial impact on the localization of near-field resonances in bow-tie antennas [15] as well as for fluorescence enhancement in plasmonic structures [16], and the selection of adhesion layer materials was shown to be critical. Due to the high electric field concentration at the corners of the nanowire waveguide, significant effects can also be expected on the transmission and polarization dependence of such waveguides. We have therefore evaluated the effect of two commonly used adhesion materials, Cr and Ti, on the propagation loss and polarization dependence in symmetric nanowire waveguides, using finite-element calculations. Part of the waveguide material was replaced by the adhesion layer material, keeping the total thickness of the structure constant. As shown in Fig. 5, the propagation loss for a 180 nm $\times$ 180 nm waveguide increases from below 2 dB/mm for the case with no adhesion layer, to about 3 dB/mm for the y-polarized mode when using a 3-nm layer of Ti or Cr. The effect, however, is less pronounced for the x-polarized mode. The PDL can be balanced, therefore, by using a slightly asymmetric structure (width $>$ height), at the cost of increased overall insertion loss.

As discussed above, the time response to thermo-optical modulation of plasmonic nanowire devices generally follows a simple model: When stepping the heating current, the power dissipation will change instantly but the waveguide core temperature will change in accordance with the heat capacity and thermal resistance to the heat sink (silicon substrate). Effectively, this is an exponential decay towards steady-state. The time constant of this thermal time response is in the sub-millisecond range, as shown in the following section. However, the BCB polymer also demonstrates a time-dependent thermo-optical memory effect (hysteresis), where the refractive index is a function of both present and past temperature. This effect is observed when bringing a VOA from the off-state up to a high-extinction state and then back (Fig. 6). The magnitude of the effect grows with the maximum temperature and the time constant of relaxation, back to the original starting point, is of the order of several hours. The plasmonic VOA functionality relies on having a negative thermo-optic coefficient. Many optical polymers are available for realizing plasmonic VOA's, and proper care

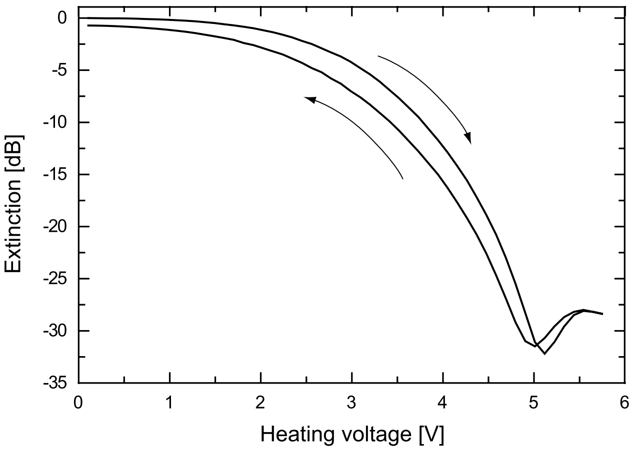

Fig. 6 Measured thermo-optical memory effect in BCB polymer. A plasmonic VOA heated to achieve >30 dB extinction exhibits a slowly reversible refractive index change when returned to the off-state

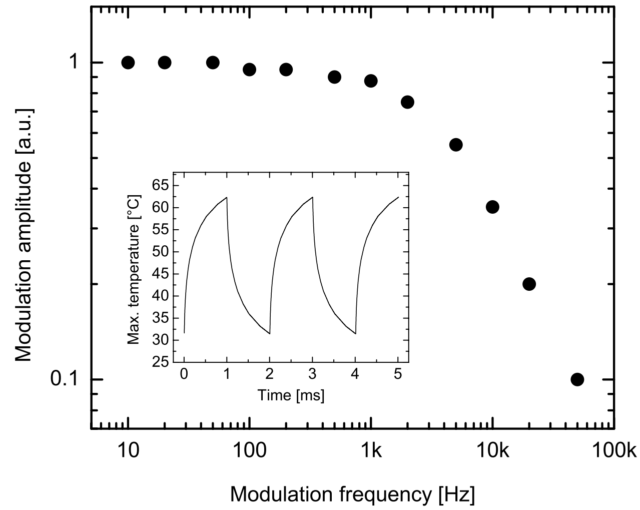

Fig. 7 Measured frequency response of the plasmonic nanowire attenuator/modulator for a fixed driving voltage amplitude (2 V). The inset shows the simulated temperature transients in the vicinity of the wire for a 0.5 kHz modulation, with the extent of the *y*-axis corresponding to full modulation

must be taken when selecting cladding materials to ensure proper thermal characteristics, stability, etc.

In general, the structural quality of the metallic waveguides is of central importance for ensuring low polarization dependence, low scattering loss, and long lifetime (limited by electromigration effects, which will be the subject of a separate publication).

7 Response time

As with other thermo-optic components, the time response of the plasmonic VOA device discussed here is limited by heat transfer. We performed simulations of thermal transients upon switching the device from the on-state to the off-state. Results were compared with measurements of the modulation of the optical signal as a function of frequency for a fixed-amplitude square-wave driving signal. Calculations show 1–2 ms heat transients which agrees well with the observed modulation roll-off at around 1 kHz, see Fig. 7. Small-signal modulation up to 100 kHz is possible at reduced output power, making the device suitable for, e.g., low-frequency pilot-tone generation (for channel labeling). Improved heat conduction from the core, e.g. through reduction of cladding thickness, will increase the bandwidth of the device but the power consumption for full modulation will simultaneously increase. The optimum trade-off will depend on the particular application of the device.

8 Conclusions

In summary, we have shown that plasmonics can play a role in integrated optics outside the nanophotonic regime, by providing an efficient method of thermo-optic control of guided signals. To be fully competitive with existing technologies, however, the main fabrication challenge lies in highly accurate patterning of metallic nanostructures. With the current rapid improvements in nanoscale fabrication techniques and the importance of high-quality metallic nanostructures for plasmonics in general, these challenges might well be overcome in the near future.

Acknowledgements The project was supported by the Icelandic Research Fund (grant no. 00700221021) and the Eimskip Research Fund.

References

1. T.W. Ebbesen, C. Genet, S.I. Bozhevolnyi, Phys. Today **61**, 44 (2008)
2. P. Berini, Opt. Lett. **24**, 1011 (1999)
3. T. Nikolajsen, K. Leosson, I. Salakhutdinov, S.I. Bozhevolnyi, Appl. Phys. Lett. **82**, 668 (2003)
4. P. Berini, Adv. Opt. Photon. **1**, 484 (2009)
5. A. Boltasseva, S.I. Bozhevolnyi, T. Nikolajsen, K. Leosson, J. Lightwave Technol. **24**, 912 (2006)
6. K. Leosson, T. Rosenzveig, P.G. Hermannsson, A. Boltasseva, Opt. Express **16**, 15546 (2008)
7. L. Eldada, R. Norwood, R. Blomquist, L.W. Shacklette, M.J. McFarland, in *Proc. Optical Fiber Communication Conf.* (2000), p. W124
8. P. Berini, Optical waveguide structures. U.S. Patent 6,741,782 2004
9. K. Leosson, T. Nikolajsen, A. Boltasseva, S.I. Bozhevolnyi, Opt. Express **14**, 314 (2006)
10. J. Jung, T. Søndergaard, S.I. Bozhevolnyi, Phys. Rev. B **76**, 035434 (2007)
11. P.B. Johnson, R.W. Christy, Phys. Rev. B **6**, 4370 (1972)

12. T. Rosenzveig, P.G. Hermannsson, K. Leosson, Plasmonics **5**(1), 75–77 (2010)
13. T. Nikolajsen, K. Leosson, S.I. Bozhevolnyi, Opt. Commun. **244**, 455 (2005)
14. M. Rashidi-Huyeh, B. Palpant, Phys. Rev. B **74**, 075405 (2006)
15. X. Jiao, J. Goeckeritz, S. Blair, M. Oldham, Plasmonics **4**, 37 (2009)
16. H. Aouani, J. Wenger, D. Gerard, H. Rigneault, E. Devaux, T.W. Ebbesen, F. Mahdavi, T. Xu, S. Blair, ACS Nano **3**, 2043 (2009)